

SELECTIVE WET-ETCHING OF AMORPHOUS/CRYSTALLIZED
Sb–Se THIN FILMS

O. Shiman, V. Gerbreder, E. Sledevskis, A. Bulanovs

Innovative Microscopy Center, Daugavpils University,
1 Parades Str., Daugavpils, LV-5400, LATVIA
e-mail: osimane@gmail.com

The paper is focused on the development of an *in situ* real-time method for studying the process of wet chemical etching of thin films. The results of studies demonstrate the adequate etching selectivity for all thin film Sb_xSe_{100-x} ($x = 0, 20, 40, 50, 100$) compositions under consideration. Different etching rates for the as-deposited and laser exposed areas were found to depend on the sample composition. The highest achieved etching rate was 1.8 nm/s for $Sb_{40}Se_{60}$ samples.

Key words: *chalcogenide thin film, amorphous and crystalline phases, etching rate.*

1. INTRODUCTION

Chalcogenide glasses are highly promising materials because of their unique physical and chemical properties. One of the most studied (see, e.g. [1, 2]) phenomena in these glasses is based on a photoinduced change in the physically-chemical properties on exposure to bandgap light (typically in the visible or near infrared (NIR) spectral region). The Se–Sb glasses have been proved to be an attractive candidate in optical and electronic communications, switching & memory devices, and photovoltaic applications. These materials can be used as data storage media. The phase resulted from high-speed transformation from “amorphous” to “crystalline” state has been widely studied as a suitable medium both for erasable [3] and WORM [4, 5] applications. In this vein, the creation of micro- and nano-scaled thin film samples becomes especially interesting and important.

Apart from that, selective etching of chalcogenide thin films in organic solution is of importance in microphotolithography, where chalcogenide films could be used as inorganic photoresist [6]. The utilization of chalcogenide thin films in gray-scale lithography is based on different dissolution rates of exposed and unexposed parts of a film. To obtain a high-quality film the dissolution rate should be different for its exposed and unexposed areas; also, a high contrast of the resist [7] is required.

To the selective wet-etching of amorphous/crystallized phases a number of articles are devoted [6-10]. The extended study of chemical etching process in $Sb_{20}Se_{80}$ thin films is described in work [11], which deals with selective wet-etching of optically and thermally crystallized/amorphous Sb_xSe_{100-x} thin films in organics-based solution (e.g. amines).

2. EXPERIMENTAL

$\text{Sb}_x\text{Se}_{100-x}$ ($x = 0, 20, 40, 50, 100$) thin films were prepared by thermal evaporation from bulk glass samples as shown in [12]. The composition and structure of the deposited layers were analyzed using an *INCA* x-act detector and a *SmartLab Rigaku* X-ray diffractometer. The optical microscopy was employed to study the modification induced by light treatment of Sb–Se samples. The topography of the structures drawn on the substrate was determined using an Atomic Force Microscope (AFM) *Veeco CP II* in the tapping mode.

The local optical crystallization of Sb–Se thin films was carried out using a He–Ne laser ($\lambda = 633$ nm, output energy 600 W/cm²) for 30 min. The organics-based solution (amines) was used for selective etching of optically crystallized/amorphous thin films. The non-stirred etching solution was kept at laboratory temperature during the etching. Real-time *in-situ* monitoring of the chemical etching process was performed according to the contactless method described in [11].

3. RESULTS

The amorphous nature of as-deposited Sb–Se thin films has been confirmed by the absence of peaks in the X-ray diffraction pattern (Fig. 1a). It is well known that heating as well as laser irradiation of Sb–Se films results in crystallization of the amorphous regions [11, 13, 14].

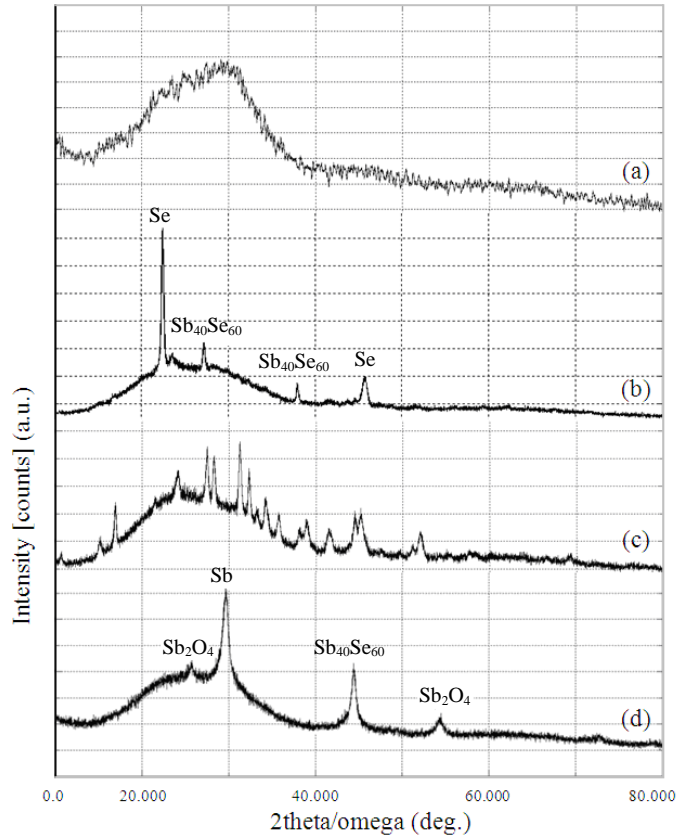


Fig. 1. X-ray diffraction patterns for as-deposited Sb–Se thin film (a), and $\text{Sb}_{20}\text{Se}_{80}$ (b), $\text{Sb}_{40}\text{Se}_{60}$ (c), $\text{Sb}_{50}\text{Se}_{50}$ (d) thin films after laser treatment. All peaks on (c) curve were identified as a $\text{Sb}_{40}\text{Se}_{60}$ crystalline structure.

In our experiment, after laser exposure the Se and $\text{Sb}_{40}\text{Se}_{60}$ crystallites were produced in the samples with an excess of selenium, while in those with a stoichiometric Sb/Se ratio only $\text{Sb}_{40}\text{Se}_{60}$ crystallites were obtained. The X-ray diffraction pattern of a sample with an excess of antimony revealed the presence of $\text{Sb}_{40}\text{Se}_{60}$, Sb and Sb_2O_4 in the crystalline phase (Fig.1 *b, c, d*). The crystallized area should be sufficient to allow clear and unambiguous X-ray diffractograms to be obtained, so laser beam passage was arranged through a diverging lens.

In the experiment, we developed the contactless method for thermally crystallized/amorphous $\text{Sb}_{20}\text{Se}_{80}$ thin films that had been used in our previous study [11], with a good etching selectivity achieved. Very high etch selectivity was detected in $\text{Sb}_{40}\text{Se}_{60}$ and $\text{Sb}_{50}\text{Se}_{50}$ samples, with the amorphous part completely dissolved and the crystallized one practically insoluble. The intensity of the reflected signal remained almost unchanged. For Sb–Se thin films the dissolution rate differences between amorphous and crystalline phases are connected with the structural changes due to illumination. The results show a pronounced decrease in the etching rate with an increase in the degree of crystallinity up to the zero rate for the crystalline phase [11]. Figure 2 shows the interference pattern of $\text{Sb}_x\text{Se}_{100-x}$ ($x = 0, 20, 40, 50, 100$) thin films experimentally obtained upon the etching process.

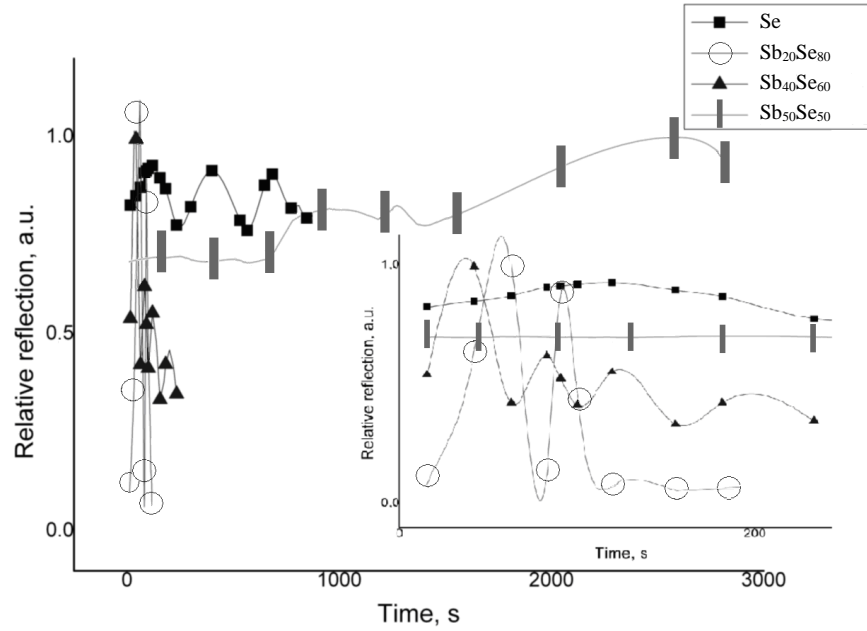


Fig. 2. Time-dependent reflected signal during the etching of amorphous $\text{Sb}_x\text{Se}_{100-x}$ thin films.

Pure amorphous selenium is etched evenly, whilst pure antimony cannot be etched even in the amorphous phase. The etching rate can be calculated as

$$v = \frac{d}{\tau},$$

where d is the thickness of deposited layer, τ is the time of complete dissolution.

The calculations have shown dependence of the etching rate on the Sb/Se ratio in the samples. The etching rate of amorphous selenium without Sb impurities is 0.4 nm/s; this value increases with addition of antimony in the composition and reaches maximum at the stoichiometric ratio ($v_{\max} = 1.8$ nm/s). Further increase in the Sb content leads to a sharp decrease in the rate of etching. Pure amorphous antimony is insoluble (Fig. 3).

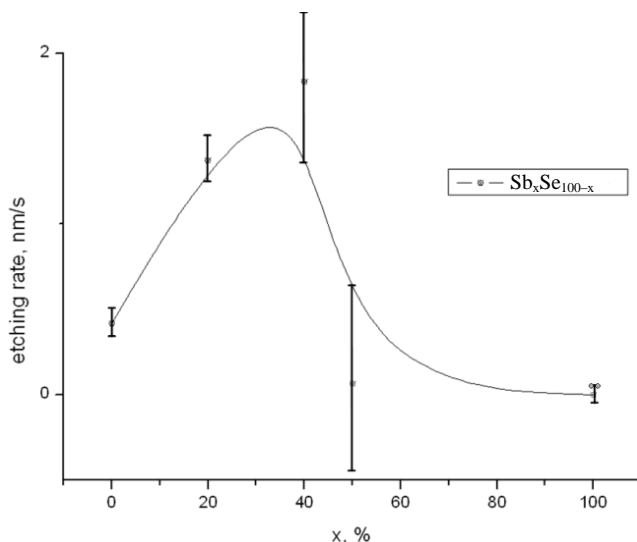


Fig. 3. Dependence of the etching rate on at.% Sb for Sb_xSe_{100-x} thin films.

4. DISCUSSION

In the experiment, the amorphous part in selectively etched locally optically crystallized/amorphous thin films was completely dissolved, whilst the laser-crystallized area turned out to be practically insoluble. The etching rate of amorphous Sb_xSe_{100-x} increases with increasing antimony content up to the stoichiometric ratio, and then abruptly drops to zero.

This indicates that the selected etchant most actively operates on Sb–Se bonds. Bonds of the kind dominate in $Sb_{40}Se_{60}$ samples, so the etching process occurs there most rapidly. In $Sb_{20}Se_{80}$ compound, apart from Sb–Se bonds there are also Se–Se bonds, for which the selected etchant is less active. The etchant does not affect Sb–Sb bonds appearing in the samples with excessive antimony, so a pure Sb sample remains insoluble.

Selective etching is a highly efficient method for the microscale element fabrication; therefore, a deeper investigation into the interaction between the etching solution and the material should be done. The different dissolution rates for amorphous and crystalline phase are also to be used in order to stabilize the phase change type recording applied in DVD technique and obtain a new type of memory. Rather smooth and homogeneous surface of the samples after the photo-stimulation and etching process as well as fine crystalline structure makes the $Sb_{40}Se_{60}$ composition attractive and promising for micro- and even nano-scale lithography.

5. CONCLUSIONS

Sb–Se thin films have been locally crystallized by laser irradiation followed by etching in organics-based solution (amines). In all cases the amorphous region was etched off, while the crystalline one remained insoluble. The etching rate was found to depend on the antimony percentage in the compound. The etching rate increases with increasing Sb amount up to the stoichiometric ratio. A further increase in the antimony content leads to a sharp decrease in the etching rate (down to zero). Based on the results obtained we can conclude that the $\text{Sb}_{40}\text{Se}_{60}$ compound is suitable for commercial fabrication of diffractive optical elements to be used in recording media for holography.

Application of selective etching could be expected in the field of micro-optical elements – grids, waveguides, microlenses, highlighting phase change type recording memories, etc..

ACKNOWLEDGEMENTS

The authors thank a colleague from the Institute of Solid State Physics J. Teteris for providing the etchant.

This work was supported by ESF (project „Atbalsts Daugavpils Universitātes doktora studiju īstenošanai”, Nr. 2009/0140/IDP/1.1.2.1.2/09/IPIA/VIAA/015).

REFERENCES

1. Stronski, A.V., Vlcek, M., Sklenar, A., Shepeljavi, P.E., Kostyukevich, S.A., & Wagner, T. (2000). Application of $\text{As}_{40}\text{S}_{60-x}\text{Se}_x$ layers for high efficiency grating production. *J. Non-Cryst. Solids*, 266–269 (2), 973–978. DOI: 10.1016/S0022-3093(00)00032-6.
2. Vlcek, M., Prokop, J., Frumar, M. (1994). Positive and negative etching of As–S thin layers. *Int. J. Electr.* 77 (6), 969–973. Retrieved from http://www.lehigh.edu/imi/Chalcogenide_Glasses/ChG11_Ref-261_Kovalskiy_Lithography%20JM3.pdf.
3. Utsugi, Y. (1993). Chemical modification for nanolithography using scanning tunneling microscopy. Nanotechnology – International Workshop on Atoms and Clusters (WAC-92); 1992 Jan 8; Atami, Japan. 1992 Oct. 161-3. *Precision Engineering*, 15 (3), 201–201. DOI:10.1016/0141-6359(93)90034-8.
4. Tokushuku, N., Moritani, K., Yanagihara, H., Konishi, K., & Noro, Y. (1992). High C/N recording in $\text{Sb}_2\text{Se}_3/\text{Bi}$ write-once disk. *Jpn. J. Appl. Phys.*, 31, 456–460. Retrieved from <http://cat.inist.fr/?aModele=afficheN&cpsidt=5266186>.
5. Barton, R., Davis, C.R., Rubin, K., & Lim, G. (1986). New phase change material for optical recording with short erase time. *Appl. Phys. Lett.*, 48 (19), 1255–1257. <http://dx.doi.org/10.1063/1.97031>.
6. Orava, J., Wagner, T., Krbal, M., Kohoutek, T., Vlcek, M., Benes, L., Kotulanova, E., Bezdicka, P., Klapetek, P., & Frumar, M. (2007). Selective wet-etching of amorphous/crystallized Ag–As–S and Ag–As–S–Se chalcogenide thin films. *J. Phys. Chem. Solids*, 68 (5–6), 1008–1013. DOI: 0.1016/j.jpcs.2007.03.056.
7. Orava, J., Wagner, T., Krbal, M., Kohoutek, T., Vlcek, M., & Frumar, M. (2006). Selective wet-etching of undoped and silver photodoped amorphous thin films of chalcogenide glasses in inorganic alkaline solutions. *J. Non-Cryst. Solids*, 352 (9–20) 1637–1640. DOI: 10.1016/j.jnoncrysol.2005.09.041.
8. Orava, J., Wagner, T., Krbal, M., Kohoutek, T., Vlcek, M., Klapetek, P., & Frumar, M. (2008). Selective dissolution of $\text{Ag}_x(\text{As}_{0.33}\text{S}_{0.67-y}\text{Se}_y)_{100-x}$ chalcogenide thin films. *J. Non-Cryst. Solids*, 354 (2–9), 533–539. DOI: 10.1016/j.jnoncrysol.2007.07.058.

9. Orava, J., Wagner, T., Krbal, M., Kohoutek, T., Vlcek, M., & Frumar, M. (2007). Selective wet-etching and characterization of chalcogenide thin films in inorganic alkaline solutions. *J. Non-Cryst. Solids*, 353 (13–15), 1441–1445. DOI: 10.1016/j.jnoncrysol.2006.10.069.
10. Vlcek, M., Schroeter, S., Čech, J., Wágner, T., & Glaser, T. (2003). Selective etching of chalcogenides and its application for fabrication of diffractive optical elements. *J. Non-Cryst. Solids*, 326–327, 515–518. DOI: 10.1016/S0022-3093(03)00463-0.
11. Shiman, O., Gerbreder, V., Sledevskis, E., Bulanovs, A., & Pashkevich, V. (2011). Selective Wet-Etching of Amorphous/Crystallized Sb₂₀Se₈₀ Thin Films. *International J. of Eng. and Applied Sci.*, 7 (2), 820–823. Retrieved from <http://www.waset.org/journals/waset/v75/v75-147.pdf>.
12. Gerbreder, Vj., Teteris, J., Sledevskis, E., & Bulanovs, A. (2007). Photoinduced changes of optical reflectivity in As₂S₃–Al system. *J. Optoelectron Adv. Mater.*, 9, 3153–3156.
13. Shiman, O., Gerbreder, V., Sledevskis, E., & Bulanovs, A. (2011). Electric conductivity of Sb/Se thin film micro-scale structures. *Latv. J. Phys. Tec. Sci.*, 48 (1), 62–68. DOI: 10.2478/v10047-011-0006-9.
14. Rubish, V.M., Shtets, P.P., Rubish, V.V., Semak, D.G., & Tszih, B.R. (2003). Optical media for information recording based on amorphous layers of Sb-Se-In system. *J. Optoelectronics Adv. Mat.*, 5, 1193–1197.

AMORFAS UN KRISTALIZĒTAS Sb–Se PLĀNĀS KĀRTIŅAS SELEKTĪVĀ ĶĪMISKĀ KODINĀŠANA

O. Šimane, V. Gerbreder, Ē. Sļedevskis, A. Bulanovs

K o p s a v i l k u m s

Nanostruktūru veidošanās dažādos materiālos ir viens no mūsdienu pētniecības galvenajiem jautājumiem. Stiklveidīgo materiālu petīšana ir īpaši interesanta un perspektīva divu iemeslu dēļ. Pirmkārt, kontrolēta nanoizmēru struktūru iegūšana stiklveidīgos materiālos jau var tikt uzskatīta par pētījumu objektu. Kā zināms, monokristāliskos materiālos mēs varam iegūt atomāri līdzēnas virsmas. Amorfos materiālos šādas manipulācijas ar atomiem ir bezjēdzīgas, jo amorfās struktūras atomu līmenī ir nesakārtotas. Otrkārt, amorfās nanostruktūras ir daudzveidīgākas nekā kristāliskās, jo nav ierobežojumu, kas saistīti ar saišu klātbūtni kristāliskā struktūrā. Tāpēc stiklveidīgie halkogenīdu pusvadītāji ir pievilcīgi materiāli nanostruktūru īpašību pētījumiem.

Šajā rakstā tiek aprakstīti halkogenīdu plānās kārtiņas kodināšanas procesu pētījumu rezultāti. Tiek parādīta paraugu augstā selektīvā spēja amorfis/kristāliskis stāvoklī: visos gadījumos (visiem sastāviem) amorfais apgabals tika nokodināts, bet kristāliskais palika neizšķīdināts. Sastāva kodināšanas ātrums ir atkarīgs no antimona procentuālā satura: palielinot antimona daudzumu līdz stehiometriskai attiecībai, arī kodināšanas ātrums palielinās. Tālāks antimona daudzuma palielinājums sastāvā noved pie strauja kodināšanas ātruma samazinājuma līdz pat nullei.

21.02.2012.